A Laboratory Study of Anisotropic Geomaterials Incorporating Recent Micromechanical Understanding

L.-T. YANG[1], X. LI[2], H.-S. YU[3], D. WANATOWSKI[4*]

1 PhD student, Nottingham Centre for Geomechanics, Faculty of Engineering, University of Nottingham, University Park, Nottingham, NG7 2RD, United Kingdom, alanyang0907@gmail.com

2 Lecturer, Fluids and Particle Processes Group, Manufacturing and Process Technologies Research Division, Faculty of Engineering, University of Nottingham, University Park, Nottingham, NG7 2RD , United Kingdom, xia.li@nottingham.ac.uk

3 Professor of Geotechnical Engineering, Nottingham Centre for Geomechanics, Faculty of Engineering, University of Nottingham, University Park, Nottingham, NG7 2RD, United Kingdom, hai-sui.yu@nottingham.ac.uk

4* Associate Professor, Department of Civil Engineering, Faculty of Science and Engineering, University of Nottingham Ningbo China, Ningbo 315100, China, d.wanatowski@nottingham.edu.cn **(Corresponding author)**.

Abstract:

This paper presents an experimental investigation revisiting the anisotropic stress-strain-strength behaviour of geomaterials in drained monotonic shear using Hollow Cylinder Apparatus. The test program has been designed to cover the effect of material anisotropy, pre-shearing, material density and intermediate principal stress on the behaviour of Leighton Buzzard sand. Experiments have also been performed on glass beads to understand the effect of particle shape. This paper explains phenomenological observations based on recently acquired understanding in micromechanics, with attention focused on strength anisotropy and deformation non-coaxiality, i.e., non-coincidence between the principal stress direction and the principal strain rate direction. The test results demonstrate that the effects of initial anisotropy produced during sample preparation is significant. The stress-strain-strength behaviour of the specimen shows strong dependence on the principal stress direction. Pre-loading history, material density and particle shape are also found to be influential. In particular, it was found that non-coaxiality is more significant in preloaded specimens. The observations on the strength anisotropy and deformation non-coaxiality were successfully explained based on the Stress-Force-Fabric relationship. It was observed that intermediate principal stress parameter b ($b = (\sigma_2 - \sigma_3)/(\sigma_1 - \sigma_3)$) has a significant effect on the non-coaxiality of sand. The lower the b-value, the higher the degree of non-coaxiality is induced. Visual inspection of shear band formed at the end of HCA testing has also been presented. The inclinations of the shear bands at different loading directions can be predicted well by taking account of the relative direction of the mobilized planes to the bedding plane.

Keywords: Anisotropy; Discrete elements; Laboratory tests; Numerical models; Plasticity; Sand (soil type).

1 Introduction

Shear strength is a fundamental soil property used in geotechnical design. Thus it must be determined with reasonable accuracy. However, the stress-stain-strength behaviour of most sedimentary deposits is anisotropic. Soil strength is generally lower when the loading is farther away from the deposition direction. Hence, soil anisotropy has attracted long-lasting interest of researchers and practitioners.

Arthur and Menzies (1972) reviewed several early studies on the soil anisotropy. They prepared samples in a tilting mould to give different directions of sample deposition with respect to the applied principal stress directions, and found the specimen produced by pouring through air in one direction corresponded to a strength and pre-failure stress-strain anisotropy. Various laboratory testing devices have been developed and applied to study soil anisotropy, including plane-strain apparatuses (e.g. Oda et al. 1978; Tatsuoka et al. 1990, Alshibli and Sture 2000; Wanatowski and Chu 2006), directional shear cells (Phillips and May 1967; Oda and Konishi 1974a, b; Wong and Arthur 1985), true triaxial apparatuses (Arthur and Menzies 1972; Yamada and Ishihara 1979; Ochiai and Lade 1983; Miura and Toki 1984; Abelev and Lade 2004) and hollow cylinder apparatuses (e.g., Symes et al. 1988; Miura and Toki 1986; Vaid et al. 1990; Gutierrez et al. 1991; Nakata et al. 1998; Rolo 2003; Lade et al. 2008; Cai et al. 2013).

Amongst available apparatuses, the hollow cylinder apparatus (HCA) that offers independent control of the magnitudes of three principal stresses and the inclination of the major-minor principal stress axes has become most popular. Extensive phenomenological observations on soil strength and loading path dependence have been made in HCA (Nakata et al. 1997; Miura and Toki 1986; Gutierrez et al. 1991; Lade et al. 2008; Cai et al. 2013). Clear evidence of material deformation non-coaxiality, an interesting phenomenon firstly reported by Roscoe

(1967) as the non-coincidence of the principal strain rate directions and the principal stress directions has been obtained from HCA testing (e.g. Gutierrez et al. 1991; Cai et al. 2013).

Based on laboratory observations, a number of advanced constitutive models have been developed, e.g., bounding surface hypoplasticity model (Li and Dafalias 2004; Lashkari and Latifi 2008; Yang and Yu 2012), yield vertex model (Tsutsumi and Hashiguchi 2005), double shearing model (Zhu 2006 a, b), yield vertex and double shearing model (Yu 2008). A state parameter has been introduced in the models to quantify the effect of material anisotropy, and often for simplicity, it is assumed that material anisotropy remains unchanged during the process of loading even though induced anisotropy has been noticed as early as in 1940's (Casagrande and Carrillo 1944).

During the last few decades, researchers have been exploring the micromechanics of soil anisotropy through multi-scale investigations. It is now generally recognized that the material anisotropy is originated from particle scale as a consequence of particle spatial arrangement, also known as the internal structure. Experimental techniques including photo-elastic testing (Oda and Conishi 1974a, b; Oda et al. 1985) and X-Ray computer tomography (Bésuelle et al. 2006; Takemura et al. 2007) have been employed to obtain particle-scale information. Computer simulations, mostly using discrete element methods (DEM), have been used as an alternative and powerful approach to explore micromechanics along with other experimental works (e.g. Cundall et al. 1982; Rothenburg and Bathurst 1989; Cambou et al. 1995).

More recently, a series of studies have been carried out at the Nottingham Centre for Geomechanics (NCG) in the UK to investigate the anisotropic stress-strain-strength behaviour of granular materials. Li and Yu (2009) presented 2D DEM simulation results that gave insight into strength anisotropy and deformation non-coaxiality. Li and Yu (2013b) explained the micromechanics with the aid of the established Stress-Force-Fabric (SSF)

relationship of granular materials (Li and Yu 2013a). The material strength and the degree of non-coaxiality were determined analytically in terms of a fabric tensor characterizing the anisotropy of material internal structure and contact force distributions characterizing the anisotropy of particle interactions (Li and Yu 2013b).

However, it is worth pointing out that laboratory testing remains an irreplaceable approach when studying fundamental behaviour of real geomaterials. Idealization of particle shapes, limitation of sample size and use of simple contact models are often inevitable in multi-scale studies. Micromechanically established theories have to be carefully validated by laboratory testing before applying to problems involving real geomaterials. Based on this context, a comprehensive experimental investigation has been carried out in this study by means of HCA to revisit the anisotropic behaviour of geomaterials. This paper offers a wide range of experimental data and evidence of some peculiar aspects of soil behaviour under monotonic loading conditions taking into account the effects of the inherent and induced anisotropy, density and particle shape, combined influence of the rotation of principal axes as well as the intermediate principal stress. The experimental data on natural sand are particularly important for development and refinement of advanced constitutive models, while the tests on glass beads will have an impact on specific numerical simulations at the particle-scale level based on discrete element modelling (DEM). In addition to the phenomenological observations, a great attention has been placed on applying recently acquired micromechanical theories to understanding the strength anisotropy and deformation non-coaxiality observed in real geomaterials.

2 Apparatus and Test Procedures

2.1 Hollow cylinder apparatus

In this study, the hollow cylinder apparatus, developed by GDS (Geotechnical Digital Systems) Instruments Ltd, was used. A schematic cross section of the GDS HCA is shown in Fig. 1. The cell contains the hollow cylindrical specimen with inner radius of 30 mm, outer radius of 50 mm and height of 200 mm. The specimen is subjected to axial load W, torque M_T, inner cell pressure p_i and outer cell pressure p_o. The axial load and displacement are generated and controlled by a high power brush servomotor attached to the base of the ball screw. Rotation of the principal stress direction is achieved by means of second servomotor attached to the splined shaft, which generates torque or angular displacement as required. The outer pressure, the inner pressure and the back pressure are controlled and/or measured by three digital pressure/volume controllers (DPVC) of 2MPa/200cc capacity. The axial load and the torque are monitored by a submersible load/torque cell attached rigidly to the cell top. The pore pressure is measured using an external pore pressure transducer connected to the base pedestal. The axial displacement and the rotation are measured by digital encoders mounted in the actuator unit.

In monotonic shear, the application of axial load W, torque M_T, inner cell pressure p_i and outer cell pressure p_o enables the control of four stress components, axial stress σ_z, radial stress σ_r, circumferential stress σ_θ, and shear stress $\sigma_{\theta z}$, on an element in the wall of the hollow cylindrical specimen. The radial strain ε_r, circumferential strain ε_θ and shear strain $\gamma_{\theta z}$ were measured indirectly from the changes of inner and outer radii of the specimen. The radius changes were computed from the changes of the volume in the inner chamber and the specimen measured by the two DPVCs. The stresses and strains are calculated following the formulations of Hight et al. (1983). The stress ratio η used in this paper was defined as the ratio of deviatoric stress q to effective mean stress p'.

HCA tests often suffer from the occurrence of stress non-uniformities across the wall of the hollow cylindrical sample as a consequence of specimen geometry, end restraints during the application of torque and different internal and external pressures. By a thorough review of numerous previous studies on the stress non-uniformities in hollow cylinder specimens, Rolo (2003) concluded that the most severe cases of non-uniformities are confined to the space where the difference between p_o and p_i is large. In order to minimize the sample non-uniformity, the experimental program was designed in the limited range of the ratio between the outer and inner cell pressures $0.9 \leq p_o/p_i \leq 1.2$, as suggested by Height et al. (1983). With regard to the sample geometry, Rolo (2003) suggested that for a given diameter, increasing sample's wall thickness increases the level of non-uniformity. An aspect ratio of H (height) / OD (outer diameter) $\geq$ 1.8 was suggested to provide end restraint free conditions. In the present study, this condition was well satisfied with aspect ratio of H / OD = 2.0, and in this respect the non-uniformity is considered less significant.

2.2 Tested materials and sample preparation

Leighton Buzzard (Fraction B) sand and Ballotini glass beads were tested in this study. Leighton Buzzard sand is standard sand consisting mainly of sub-rounded quartz particles with some carbonate materials. The Ballotini glass beads are made of high quality pure soda-lime glass. The index properties of the two materials are summarized in Table 1. Scanning electron micrographs of Leighton Buzzard sand and Ballotini glass beads are shown in Fig. 2(a) and (b), respectively.

The water sedimentation method was used to prepare all the samples. This method mimics natural depositional environment satisfactorily and enables preparation of relatively homogeneous reconstituted sand samples with controlled density (Wanatowski and Chu 2008). To ensure high saturation of specimens, de-aired water was flushed throughout the

specimen. The specimen was left overnight with a back pressure of 400 kPa and outer and inner cell pressures of 420 kPa. The specimen was considered satisfactorily saturated when Skempton's B-value was greater than 0.96. The outer and inner cell pressures were then increased to 600 kPa with the constant back pressure of 400 kPa. Hence, all the specimens were isotropically consolidated to the effective confining pressure p' = 200 kPa.

2.3 Experimental program

Each series of drained monotonic shear tests with various loading directions carried out in this study are summarized in Table 2. The first two series of tests were performed on dense and medium dense Leighton Buzzard sand in order to generate a basic understanding of the anisotropic behaviour of granular geomaterials. All the samples in Series 1 and 2 were sheared in a drained condition with various principal stress directions, as shown in Fig. 3. The results from these series of tests were used as a reference for comparison with the other series of tests. The third series of tests were performed on presheared sand specimens in order to investigate the impact of preshearing on the response of sand to subsequent loading. In this series of tests, a presheared specimen was obtained by shearing the isotropically consolidated specimen in the vertical direction (α = 0°) up to the peak and unloading it to a stress state with deviatoric stress q = 20kPa (see Fig. 4). It was observed that at the peak stress, the volumetric dilation of the specimen was less than 1% and the geometry of the specimen had no significant change based on visual inspection. Therefore, the specimen can be considered as uniform before reloading. The fourth series of tests was performed on dense sand with various combinations of α and b. The emphasis of this test series was placed on investigating the combined effects of principal stress direction and intermediate principal stress. Finally, the fifth series of tests was performed on glass beads in order to study the effect of particle shape on the behaviour of granular materials. As shown in Table 2, each series of tests are

labelled in such a way that the first two letters indicate the type of material and the third letter indicates material density followed by investigated testing parameters.

Fig. 3 illustrates the stress paths in the *X-Y* stress space for monotonic loading tests with different inclinations of the major principal stress (α = 0°, 15°, 30°, 60°, 75°, and 90°). During the tests, monotonic loading was applied in HCA strain-controlled mode in terms of the axial displacement under drained conditions. To ensure full discharge of water from the specimen, the axial strain was increased at a slow rate of 0.05%/min. In all the tests the value of the mean effective stress *p'* and the value of the intermediate principal stress parameter *b* was maintained constant. It needs to be noted that due to the limitations of the HCA, the value of α cannot be accurately controlled at very low levels of deviatoric stress. Therefore, in all the tests, a deviatoric stress of 15 kPa was applied using HCA stress-controlled mode before the rotation of the major principal stress direction was implemented. It should also be pointed out that since the calculations of stresses and strains in HCA testing are based on global measuring system, the post-peak stress-strain curves could be subject to considerable error due to severe changes in sample thickness and curvature along the sample height. Nonetheless, the post-peak stress-strain behaviour remains very useful for qualitative assessment of soil behaviour and thus is included in all the plots.

3 Results and Discussions

3.1 Material anisotropy

3.1.1 Stress-strain behaviour

The first series of tests, performed on dense Leighton Buzzard sand, is shown in Fig. 5(a). The effect of anisotropy produced during sample preparation is apparent in both stress ratio and volumetric strain responses. For volumetric strain shown in the figures, a positive value along the vertical axis indicates contraction and the negative indicates dilation. The shear

strength reduces and the volumetric compressibility increases with increasing values of α. The highest peak was obtained when the major principal stress direction was vertical and it was reduced dramatically as the direction of the major principal stress was changed from α = 30° to α = 60°. Similar observations have been reported by Arthur and Menzies (1972) in cubical triaxial tests on tilted samples, Oda et al. (1978) in plane strain tests, Arthur et al. (1981) in directional shear cell tests and Cai et al. (2013) in HCA tests.

The impact of preshearing on the material response to sub-sequential loading has been investigated by comparing test results on samples with and without preloading histories as shown in Fig. 5(a) and 5(b). Both figures demonstrate dependence of stress-strain behaviour on the direction of principal stress axes α for monotonic shear tests from test series LBD and LBD-PL, respectively. It is clear that the preshearing history to the peak stress has a significant effect on the subsequent stress-strain response of sand. Generally, a softer response in the stress-strain relationship, larger initial contraction and larger strain to reach the peak stress ratio were observed at each loading direction for presheared specimens.

3.1.2 Strength anisotropy

Values of the peak stress ratio η_p at different major principal stress direction α obtained from test series LBD and LBD-PL are compared in Fig. 6. It can be seen from Fig. 6 that the variation of the peak stress ratios with principal stress direction shows similar trend patterns for the two series of tests. The highest peak stress ratio was obtained when the major principal stress direction was parallel to the deposition direction (i.e. α = 0°) and the lowest value was obtained at α = 60°. The specimen strength reverted slightly from α = 60° to 90°. Similar observations are reported by Miura et al. (1986). It is interesting to see that despite significant difference in the stress-strain response between the non-presheared and presheared

specimens, the values of the peak stress ratio measured at different loading directions for the two specimens are almost the same.

Using 2D discrete element code PFC2D, Li and Yu (2009) prepared and tested anisotropic specimens consisting of non-spherical particles under monotonic loading with different fixed strain increment directions. In their simulations, an initially anisotropic sample was prepared using a deposition method and a presheared sample was obtained by shearing the initially anisotropic specimen in the deposition direction to 25% axial strain and then unloading it to the isotropic stress state. The pre-failure stress ratio (corresponding to 2% of axial strain) with different loading directions obtained from initially anisotropic samples and preloaded samples were analysed thoroughly by Li and Yu (2009). A qualitative analysis of the DEM simulations and the HCA test results from the current study shows a similar variation of the pre-failure stress ratios with different loading directions. Based on the established Stress-Force-Fabric (SFF) relationship (Rothemburg and Bathurst 1989, Li and Yu 2013a), Li and Yu (2013a) explained that when material approaches the peak stress ratio, the direction of the force anisotropy and fabric anisotropy are generally coaxial with loading direction. Therefore, the magnitude of peak stress ratio is dependent on the developed degrees of force anisotropy and fabric anisotropy. However, as the loading directions changes from $\alpha = 0°$ to 60°, the force anisotropy and fabric anisotropy decrease, leading to decreasing value of stress ratio. Upon further increase of α to 90°, the fabric anisotropy decreases continuously while the force anisotropy increases, resulting in slight increase of stress ratio. The micromechanical explanation is supported by the experimental data with the qualitative agreement with DEM simulation results.

3.1.3 Deformation non-coaxiality

The numerical study carried out by Li and Yu (2009) shows that a preloading history may have significant effects on the anisotropic behaviour of granular materials to subsequent loading. Although deformation non-coaxiality is negligible for initially anisotropic samples, it could be significant once the samples have been presheared. However, laboratory evidence based on real geomaterials has not been reported in the literature.

The major directions of stress and strain increment obtained from test series LBD and LBD-PL are plotted against the stress ratio in Fig. 7(a) and 7(b), respectively. During shearing, the direction of major principal stress α was fixed, as indicated by solid lines in Fig. 7. The calculated strain increment directions are indicated by dashed lines with open circle symbols. The results obtained from test series LBD and LBD-PL supplement the observations made by Li and Yu (2009). The degree of non-coaxiality observed in the tests conducted on presehared specimens is significantly different from that obtained from non-presheared specimens. Fig. 7(b) shows that significant non-coincidence between the stress and strain increment directions was observed at α = 15°, 30°, 60° and 75°. The deviations were especially large when α = 30° and 60°, where the degree of non-coaxiality reached about 22° in both cases. Similarly, in the 2D DEM simulations, it was found that the degree of non-coaxiality was greatly enlarged by the preshearing history to the pre-failure stress ratio and the largest deviations between the directions of stress and strain increment in the presheared specimens was about 20° at α = 60° (Li and Yu 2009). It needs to be noted that in Li and Yu's simulation (Li and Yu 2009), loading was applied in a strain-controlled mode with the principal strain direction fixed. However, by comparing the results between stress-controlled and strain-controlled monotonic loading tests, Li and Yu (2009) pointed out that loading mode does not significantly affect measured degree of non-coaxiality.

Based on the SFF relationship, Li and Yu (2013b) reported that non-coaxiality was quantitatively dependent on the relative direction, as well as the relative magnitude of the fabric anisotropy (Fig. 8 (a)) and the contact force anisotropy (Fig. 8 (b)). As the direction of force anisotropy is almost coaxial with the loading direction during shearing, non-coaxiality is the result of the principal directions of fabric anisotropy deviating from the loading direction. Microscopically, it was found that for simulation with loading direction parallel to the deposition direction ($\alpha = 90°$), the principal direction of fabric anisotropy was coincident with loading direction throughout the shearing. In the test with loading direction perpendicular to the preloading direction ($\alpha = 0°$), the principal directions of fabric anisotropy quickly approach to the loading direction at the initial stage of shearing. Hence, the material behaves almost coaxially when the samples are loaded in the direction of major principal stress parallel or perpendicular to the deposition direction. However, for simulations with loading direction fixed at $\alpha = 75°$, 60°, 45°, 30° and 15°, shown in Fig. 8 (a), the principal directions of fabric anisotropy are gradually rotated in such a manner that they finally point in the loading direction at large strain levels, thus it can be observed that the non-coaxiality degree decreases with increasing stress ratio and the granular material is nearly coaxial close to failure. As for the presheared specimens, the magnitude of fabric anisotropy was found to be larger than the initially anisotropic sample prepared by deposition. Accordingly, more significant deformation non-coaxiality was observed. Therefore, DEM simulations reported by Li and Yu (2013b) give a plausible explanation for the observations on Leighton Buzzard sand, shown in Fig 7.

3.2 Effects of material density and particle shape

It is well known that void ratio is one of the most important parameters controlling mechanical response of soils. The investigation of the effects of material density on the

anisotropic behaviour of granular materials was carried out in this study by comparing test results on dense sand (LBD) and medium dense sand (LBM).

Glass beads have long been used to study anisotropic behaviour of 'idealized' granular materials (e.g. Kallstenius and Bergau 1961; Haruyama 1981; Kuwano 1999). Their relatively simple geometry and uniform particle size distribution allowed the influence of particle shape to be examined independently. On the other hand, the application of glass beads in laboratory test provides comparable data for numerical as well as constitutive modelling of granular materials. Therefore, experiments on glass beads (GBD) were also performed in this study and the results were compared with those of sand (LBD).

Fig. 9 presents the comparison of the stress-strain curves obtained for LBD and LBM at three representative loading directions (α = 0°, 30° and 90°). For a comparison purpose, the results from LBM are plotted as solid lines while the corresponding results of LBD are shown as dashed lines. It can be observed from Fig. 9 that regardless of the loading direction, the medium dense sand tends to exhibit softer stress-strain response, lower shear strength, and more contractive volumetric strain than those of the dense sand. Moreover, larger deviatoric strain was required for the medium dense sand to reach the peak state.

The comparison of the LBD and GBD results are shown in Fig. 10 with solid lines representing GBD and dashed lines representing LBD. It can be seen from Fig. 10 that the glass beads tend to have softer stress-strain response, lower shear strength and larger volume compressibility, even though the beads have higher relative density than the sand. It is also obvious from Fig. 10 that spherical glass beads exhibit more severe fluctuations in its stress-strain curves than angular sands (also known as stick-slip phenomenon, Adjémian (2005)).

Comparison of the peak stress ratios obtained at different loading directions from test series LBD, LBM and GBD are shown in Fig 11. It can be observed that the general trend of the

variation of peak stress ratios with increasing values of α is similar for the three series of tests. However, the results obtained from test series LBD and LBM show that the maximum difference between the peak stress ratios obtained from both series is only 0.06 and it was obtained at $\alpha = 0°$, even though the difference between the relative densities of the two samples is about 34%. The difference between results obtained from test series LBD and GBD, was more significant. As shown in Fig. 11, a large reduction in the material strength was observed when the angular sand was changed to the spherical glass beads even though the relative density of the glass beads was 14% higher than the dense sand (see Table 2).

Fig. 12 shows the comparison of the calculated strain increment directions obtained at different loading directions from test series LBD, LBM and GBD. It can be seen that the magnitudes of the directions of strain increments were very similar at each loading direction for test series LBD and LBM. Therefore, the experimental results suggest that the effect of relative density on the non-coaxial behaviour of sand in monotonic shear is not significant. As indicated in Fig. 12, despite the slightly smaller degree of non-coaxiality in test series GBD, the margin by which the non-coaxiality of LBD exceeded that of the GBD was limited to 3°. Hence, the effect of particle shape on the non-coaxial behaviour of sand in monotonic shear is also not significant.

3.3 Effects of principal stress direction and intermediate principal stress

As most of the field problems in geotechnical engineering are three dimensional, a soil is more likely to be subjected to an anisotropic stress state ($\sigma_1 \neq \sigma_2 \neq \sigma_3$), together with a rotation of the principal axes. Experimental investigation on the effects of intermediate principal stress on soil behaviour has been an interesting topic in the last couple of decades (e.g. Lade and Duncan 1973; Reades and Green 1976; Ochiai and Lade 1983; Sayao and

Vaid 1996; Kumruzzaman and Yin 2010). However, to the authors' knowledge, there is very limited data obtained from drained HCA test with various combinations of principal stress direction α and intermediate principal stress parameter b. Therefore, the combined effects of α and b on the behaviour of granular materials under drained monotonic shearing were investigated in the present study.

3.3.1 Stress-strain behaviour

The stress-strain behaviour at different major principal stress directions for test series LBD-B02, LBD and LBD-B10 are presented in Fig. 13. In general, irrespective of loading directions, the material becomes increasingly soft as the b-value increases. The highest peak stress ratio was obtained when b = 0.2 and a significant decrease in material strength was observed with increasing values of b. The volumetric response also shows a consistent pattern. The volumetric compressibility of the specimens increases with increasing b-value.

For the tests with the major principal stress direction α = 0º, 15º and 30º, shown in Fig. 13 (a)-(c), the stress-strain curves become increasingly steeper with increasing b-value. For test series LBD-B10, specimens failed quickly with a sharp drop in the stress-strain curve after the peak was reached. Similarly, at different loading directions the curves also show a clear decreasing strength from b = 0 to b = 1. Comparing the volume change, all the samples tested at α = 0º, 15º and 30º show predominantly dilatant response. For test series LBD-B02 and LBD, there is no tendency for contraction. The specimens were dilating throughout the tests, as shown in Figs. 13(a)-(c). However, for test series LBD-B10, volumetric response became dilatant after the initial contraction and with further shearing, associated with strain softening.

It can be seen from Fig. 13 (d)-(f), that typical trend indicated in the tests with α = 0º, 15º and 30º can also be observed in the tests with α = 60º, 75º and 90º, that is, the stiffness and shear strength of sand reduces and the volumetric compressibility increases with increasing values

of b. Furthermore, it is apparent that the stress-strain curves obtained from test series LBD-B10 tend to be steeper than those in the other two series and they reach the peak deviator stress at lower strains. However, the pre-peak stress-strain curves of the test series LBD-B02 and LBD are very close to each other at α = 60º. Comparing the volume change curves, it is interesting to note that the difference between the volumetric strains developed in the test series LBD-B02 and LBD tends to diminish as α increases from 60º to 90º.

3.3.2 Strength anisotropy and deformation non-coaxiality

As shown in Fig. 14, the variation of the peak friction angle measured at different loading directions for the three cases of b-value investigated in this study is similar. As b-value changed from 0.2 to 0.5, the strength increases and there is a drop in strength as b further increases from 0.5 to 1.0. However, as indicated in the figure, the peak friction angles obtained at b = 1.0 gradually shifted down with the increasing value of α. For α = 0º, 15º and 30º, the lowest strength is reached at b = 0.2, whereas for α = 60º, 75º and 90º, it is obtained at b = 1.0. Above observations clearly show that both the inherent anisotropy and the intermediate principal stress may have a profound influence on the behaviour of sand with anisotropic fabric. Neglecting the effects of the soil anisotropy in the investigation of intermediate principal stress may results in inadequate interpretation of test results.

The principal strain increments calculated from test series LBD-B02, LBD and LBD-B10 at different fixed principal stress directions are compared in Fig. 15. It can be seen that there is noticeable influence of the b-value on the non-coaxiality of sand. In general, at α = 15º, 30º and 60º, the lower the b-value, the higher the degree of non-coaxiality. Test series LBD-B02 show a comparatively larger deviations between the major directions of stress and strain increment at α = 15º and α = 30º. The largest deviations between the two directions occurred

in the test series LBD-B02 at α = 15º, reaching about 15º. However, at α = 0 º, 75º and 90º all the three specimens behave almost coaxially throughout the tests.

Numerical studies based on 3D DEM have also evolved to investigate the effects of intermediate principal stress on the behaviour of initially isotropic granular materials (e.g. Thornton 2000, Thornton and Zhang 2010, Barreto and O'Sullivan 2012). However, the effect of inherent anisotropy was not considered in these simulations. The combined effects of loading direction and intermediate principal stress on the behaviour of granular materials in generalized three-dimensional stress state remain unaddressed. Hence, the fundamental understanding of the relationship between the macro- and micro-scale responses of granular materials under generalized stress conditions is not well understood.

3.4 Shear banding

After each test, the specimen was held under vacuum in order to record any shear bands that had developed during shearing. Fig. 16 presents different shear band patterns and inclination angles at different loading directions obtained from test series LBD. As shown in the figure, the angle of shear band inclination is measured from the vertical direction (centre line on the front surface of the specimen) to the direction of shear band plane on the front of the specimen.

It can be seen from Fig. 16 that bulging was observed for specimens tested with α = 0°, 15° and 30°, and necking was observed for specimens tested with α = 60°, 75° and 90°. Crossed shear bands were produced at α = 0° and 90°, and the intersections of the shear bands were mainly concentrated in the middle part of the specimen. For α = 15°, several parallel spiral shear bands were wrapped around the body of the specimen with almost equal distance between each other. For α = 30 and 75° single spiral shear bands were developed. However,

for α = 60°, specimen was twisted at the interface between the base pedestal and the specimen ends.

Based on force equilibrium, Coulomb's theory (Coulomb 1773) states that failure occurs at the point of maximum obliquity, and the inclination of shear bands therefore coincides with the inclination of planes on which the ratio of shear to normal stress reaches its maximum value (mobilized plane). In this case, the angle θ_σ between the shear band orientation and the direction of major principal strain increment can be expressed as:

$$\theta_\sigma = 45° \pm \varphi/2$$

where: φ is the friction angle

By taking the magnitude of effective major and minor principal stresses at the peak stress state, the value of φ at different loading directions was calculated and the value of the angle θ_σ could therefore be obtained. The actual shear band inclinations obtained in the experiments are compared with the theoretical predictions in Table 3. For the sake of comparison, the experimental shear band inclinations (*sb*) and theoretical predictions (Mobilized plane I and II) are sketched in Fig. 17. It can be seen that at α = 0° and 90° crossed shear bands were developed asymmetrically about the vertical direction, and they matched well with the two mobilized planes predicted by Coulomb's theory. However, in the tests with α = 15°, 30°, 60° and 75°, the shear bands were developed in just one direction, which is inconsistent with theoretical predictions. From the microscopic point of view, Miura et al. (1986) pointed that the interlocking between elongated sand particles with their long axes laid horizontally have the weakest resistance to shear stress on the bedding plane. Consequently, the specimen deforms most easily when the mobilized plane coincides with the bedding plane. By taking this anisotropic behaviour into consideration, it can be seen from Fig. 17 that for α = 15°, 30°, 60° and 75° Mobilized plane II is closer to the bedding plane than Mobilized plane I. This

means that the lowest shear resistance and largest sliding displacement will occur more likely on Mobilized plane II rather than on Mobilized plane I. The inclinations of shear bands measured in this study at different loading directions confirm Miura's theory.

Conclusions

This paper presents an experimental investigation revisiting anisotropic stress-strain-strength behaviour of geomaterials in drained monotonic shear using Hollow Cylinder Apparatus. The test program has been designed to cover the effect of material anisotropy, preshearing, material density and intermediate principal stress on the behaviour of Leighton Buzzard sand. Experiments have also been performed on glass beads to understand the effect of particle shape. Visual inspection of shear band formed at the end of testing has been presented. An attempt has also been made to explain the phenomenological observations of strength anisotropy and deformation non-coaxiality based on the recently acquired understanding in micromechanics. The major findings and conclusions can be summarized as follows:

- The effect of anisotropy produced during sample preparation is apparent in both deviatoric strain and volumetric strain responses of sand. Sand specimens subjected to preshearing to the peak stress were found to be softer and contracted more in the subsequent responses. For a given loading direction, the peak shear strength is relatively unaffected by preloading to the peak stress. However, the preshearing history does have a significant effect on the non-coaxiality of sand specimens. It was also found that lower relative density and rounder particle shape of the assembly of granular materials tend to produce softer response, severer initial contraction and lower shear strength in monotonic

shear. However, the effects of the particle shape and relative density on the non-coaxial behaviour of granular materials under monotonic shear were found to be less significant.

- Both, the loading direction and intermediate principal stress, have significant effects on the stress-strain behaviour of anisotropic sand under drained monotonic shear. For the same loading direction with constant α values, the shear strength of sand reduces and the volumetric compressibility increases with increasing values of b. The sand exhibits its highest peak friction angle at $b = 0.5$ and $\alpha = 0^{\circ}$ and the lowest at $b = 1.0$ and $\alpha = 75^{\circ}$. The influence of b-value on the non-coaxial behaviour of sand under monotonic shear is also evident. The lower the b-value, the higher the degree of non-coaxiality is induced.

- The initial anisotropy produced during sample preparation has pronounced effects on the formation of shear band in monotonic shear test. Different shear band patterns and inclination angles were observed from specimens with different loading directions. The obtained shear band inclinations were compared with theoretical predictions by Coulomb's theory. It was found that the inclinations of the shear bands at different loading directions can be predicted well by taking account of the relative direction of the mobilized planes to the bedding plane.

- The phenomenological observations of strength anisotropy and deformation non-coaxiality was explained by recently acquired micromechanical theories. Based on the established Stress-Force-Fabric relationship, the strength anisotropy of granular materials was mainly due to the differences in the variation of the degrees of fabric anisotropy and force anisotropy at different loading directions. The degree of non-coaxiality was dependent on the relative direction, as well as the relative magnitude of the fabric anisotropy and the contact force anisotropy. As in monotonic shearing, the direction of force anisotropy is coaxial with the loading direction. The deformation non-coaxiality is

hence the result of the principal directions of fabric anisotropy being deviated from the loading direction.

REFERENCES

Arthur R. F. and Menzies B.K. 1972. Inherent anisotropy in sand. *Geotechnique*, Vol. 22, No. 1, 115-131.

Arthur, J. R. F., Bekenstein, S., Germaine, J. T., and Ladd, C. C. 1981. Stress path tests with controlled rotation of principal stress direction. *Laboratory Shear Strength of Soil, American Society for Testing and Materials,* STP 740, 516-540.

Abelev, A., and Lade, P. V. 2004. Characterization of failure in cross anisotropic soils. *Journal of Engineering Mechanics*, Vol. 130, No. 5, 599-606

Alshibli, A. K. and Sture, S. 2000. Shear band formation in plane strain experiments of sand. *J. Geotech. Geoenviron. Engng,* ASCE, Vol. 126, No. 6, 495-503.

Adjémian, F. and Evesque P. 2005. Experimental stick-slip behaviour in triaxial test on granular matter. *Poudres & Grains*, Vol. 12, 115-121.

Bésuelle P., Viggiani G., Lenoir N., Desrues J., Bornert M. 2006. X-ray Micro CT for Studying Strain Localization in Clay Rocks under Triaxial Compression. *Keynote paper, in: Advances in X-Ray Tomography for Geomaterials*. J. Desrues et al. Eds, ISTE, London, 35-52.

Barreto, D. and O'Sullivan C. 2012. The influence of inter-particle friction and the intermediate stress ratio on soil response under generalised stress conditions. *Granular Matter,* Vol. 14, 505-521.

Cai, Y.Y., Yu, H. S., Wanatowski, D., and Li, X. 2013. Non-coaxial behavior of sand under various stress paths. *J. Geotech. Geoenviron. Eng.*, Vol. 139. No. 8. pp. 1381–1395.

Casagrande A. and Carrillo N. 1944. Shear Failure on Anisotropic Materials. *Proc. Boston. Soc. of Civil Eng*, Vol. 31, 74-87.

Coulomb, C.A., 1773. Sur l'application des règles des maximis et minimis à quèlquesproblèmes de statique relatifs à l'architecture. Mémoires de Mathématique et de Physique. *Académie Royale des Sciences*, Vol. 7, 343–382.

Cundall, P.A., Drescher, A. and Strack, O.D.L., 1982. Numerical experiments on granular assemblies: measures andobservations. *Deformation and Failure of Granular Materials, Balkema*, pp. 355-370.

Cambou, B., Dubujet, P., Emeriault, F. and Sidoroff, F., 1995. Homogenization for granular materials. *Eur. J. Mech. A, Solids,* Vol. 14, No. 2, 225–276.

Gutierrez, M., Ishihara, K. and Towhata, I. 1991. Flow theory for sand during rotation of principal stress direction. *Soils and Foundations*, Vol. 31, No. 4, 121-132.

Haruyama, M. 1981. Anisotropic deformation-strength properties of an assembly of spherical particles under three dimensional stresses. *Soils and Foundations*. Vol. 21, No. 4, 41-55.

Hight, D.W., Gens, A., Symes, M.J. 1983. The development of a new hollow cylinder apparatus for investigating the effects of principal stress rotation in soil. *Geotechnique*, Vol. 33, No. 4, 355-383.

Kumruzzaman, M. D. and Yin, J. H. 2010. Influences of principal stress direction and intermediate principal stress on the stress–strain–strength behaviour of completely decomposed granite. *Canadian Geotechnical Journal*, Vol. 47, No. 2, 164-179.

Kallstenius, T. and Bergau, W., 1961. Research on the texture of granular masses. *Proc. 5th Int. Conf. on Soil Mechanics and Foundation Engineering,* Vol. 1, 165-170.

Kuwano R. 1999. The stiffness and yielding anisotropy of sand. *PhD thesis submitted to the Department of Civil Engineering, the University of London.*

Lade, P.V., Duncan, J.M., 1973. Cubical triaxial tests on cohesionless soil. *Journal of the Soil Mechanics and Foundation Division*, ASCE, 99(SM10), pp. 793-811.

Lade, P.V., Nam, J., and Hong, W.P. 2008. Shear banding and cross-anisotropic behaviour observed in laboratory sand tests with stress rotation. *Canadian Geotechnical Journal*, Vol.45, 74-84.

Lashkari, A. and Latifi, M. 2008. A non-coaxial constitutive model for sand deformation under rotation of principal stress axes. *International Journal for Numerical and Analytical Methods in Geomechanics.*Vol. 32, No. 9, 1051-1086.

Li, X. and Yu H.S. 2009. Influence of loading direction on the behaviour of anisotropic granular materials. *International Journal of Engineering Science*, Vol. 47, 1284-1296.

Li, X. and Yu H.S. 2013a. Fabric, force and strength Anisotropies in granular materials: A micromechanical insight. *Accepted by Acta Mechanica*.

Li, X. and Yu H.S. 2013b. Particle scale insight into deformation non-coaxiality of granular materials. *Accepted by International Journal of Geomechanics*.

Li X. S. and Dafalias Y. F. 2004. A constitutive framework for anisotropic sand including non-proportional loading. *Geotechnique*, Vol. 54, No. 1, 41-51.

Miura, S. and Toki S. 1984. Anisotropy in mechanical properties and its simulation of sands sampled from natural deposits. *Soils and Foundations*, Vol. 24. No. 3, 69-84.

Miura, S. and Toki S. 1986. Deformations prediction for anisotropic sand during the rotation of principal stress axes. *Soils and Foundations*, Vol. 26, No.3, pp. 42-56.

Nakata, Y., Hyodo, M., Murata, H., Itakura, S. and Yamada, Y. 1997. Flow deformation of sands subjected to principal stress rotation. *Memoirs of the Faculty of Engineering, Yamaguchi University*, Vol. 48, No. 1, 57-64.

Nakata, Y., Hyodo, M., Murata, H., and Yasufuku, N. 1998. Flow deformation of sands subjected to principal stress rotation*. Soils and Foundations*, Vol. 38, No.3, 115-128.

Ochiai, H. and Lade P.V. 1983. Three-dimensional behaviour of sand with anisotropic fabric. *Journal of Geotechnical Engineering*. Vol. 109, No.10, 1313-1328.

Oda, M. and Konishi J. 1974a. Microscopic deformation mechanism of granular material in simple shear. *Soils and Foundations*, Vol.14, No. 4, 25–38.

Oda, M. and Konishi J. 1974b. Rotation of principal stresses in granular material during simple shear. *Soils and Foundations*, Vol.14, No. 4, 39–53.

Oda, M., Isao K. and Toshio H. 1978. Experimental study of anisotropic shear strength of sand by plane strain test. *Soils and Foundations*, Vol. 18, No. 1, 25-38.

Oda, M., Nemat-Naser, S., and Konishi, J. 1985. Stress-induced anisotropy in granular masses. *Soils and Foundations*. Vol. 25, No.3, 85–97.

Phillips, A. B. and May, P. H. 1967. A form of anisotropy in granular media. Special Task Report, *Dept. of Civil and Municipal Engineering, Univ. College, London.*

Roscoe, K. H., Bassett, R. H., and Cole, E. R. L., 1967. Principal axes observed during simple shear of a sand. Proc. *4th Eur. Conf. Soil Mech. Found. Eng.* Oslo, 231-237.

Reades, D. W. and Green G. E., 1976. Independent stress control and triaxial extension tests on sand. *Géotechnique.* Vol. 49, pp. 551-576.

Rolo, R., 2003. The anisotropic stress-strain-strength behaviour of brittle sediments. *PhD thesis submitted to the Department of Civil Engineering, the University of London.*

Rothenburg, L. and Bathurst, R. J. 1989. Analytical study of induced anisotropy in idealized granular materials. *Géotechnique*, Vol. 49, pp. 601-614.

Sayao, A.S.F.J., and Vaid, Y.P. 1991. A critical assessment of stress nonuniformities in hollow cylinder test specimens. *Soils and Foundations*, Vol. 31, No. 1, pp. 60-72.

Sayao, A.S.F.J., and Vaid, Y.P. 1996. Influence of intermediate principal stress on the deformation response of sand. *Canadian Geotechnical Journal*, Vol.33, 822-828.

Symes, M. J., Gens, A., and Hight, D. W. 1988. Drained principal stress rotation in saturated sand. *Geotechnique*, Vol. 38., No. 1, 59-81.

Takemura, T., Takahashi, M., Oda, M., Hirai, H., Murakoshi, A. and Miura, M. 2007. Three-dimensional fabric analysis for anisotropic material using multi-directional scanning line—application to X-ray CT image. *Materials Transactions*, Vol. 48, No. 6, 1173-1178.

Tatsuoka, F., Nakamura, S., Huang, C. C., and Tani, K. 1990. Strength anisotropy and shear band direction in plane strain tests of sand. *Soils and Foundation*, Vol. 30, No. 1, 35-54.

Tsutsumi S. and Hashiguchi K. 2005. General non-proportional loading behaviour of soils. *International Journal of Plasticity*. Vol. 22, 826-857.

Thornton, C. 2000. Numerical simulation of deviatoric shear deformation of granular media." *Géotechnique*. Vol. 50., No.1, 43-53.

Thornton, C. and Zhang, L. 2010. On the evolution of stress and microstructure during general 3D deviatoric straining of granular media. *Géotechnique*. Vol. 60, No. 5, 333-341.

Vaid, Y.P., Sayao, A.S.F, Hou, E. and Negussey, D. 1990, Generalised stress-path dependent behaviour with a new hollow cylinder torsional apparatus. *Canadian Geotechnical Journal*, Vol. 27, 601-616.

Wanatowski, D., and Chu, J. 2006. Stress-strain behavior of a granular fill measured by anew plane-strain apparatus, *Geotechnical Testing Journal*, Vol. 29, No. 2, 149-157.

Wanatowski, D., and Chu, J. 2008. Effect of specimen preparation method on the stress-strain behavior of sand in plane-strain compression tests. *Geotech. Test. J.*, Vol. 31, No. 4, 308-320.

Wong R. K. S. and Arthur R. F. 1985. Induced and inherent anisotropy in sand. *Geotechnique*, Vol. 35, No. 4, 471-481.

Yamada, Y., and Ishihara, K. 1979. Anisotropic deformation characteristics of sand under three dimensional stress conditions. *Soils and Foundations*, Vol. 19, No. 2, 79–94.

Yang Y. M. and Yu, H. S. 2012. A kinematic hardening soil model considering the principal stress rotation. *International Journal for Numerical and Analytical Methods in Geomechanics*, Vol. 37, No. 13, 2106–2134.

Yu H. S. 2008. Non-Coaxial Theories of Plasticity for Granular Materials. In: *The 12th International Conference of International Association for Computer Methods and Advances in Geomechanics (IACMAG)*, India, Goa.

Zhu, H. N., Mehrabadi M. M. and Massoudi M. 2006a. Incorporating the effects of fabric in the dilatant double shearing model for planar deformation of granular materials. *International Journal of Plasticity*. Vol. 22, 628-653.

Zhu, H. N., Mehrabadi M. M. and Massoudi M. 2006b. Three-dimensional constitutive relations for granular materials based on the dilatant double shearing mechanism and the concept of fabric. *International Journal of Plasticity*. Vol. 22, 826-857.

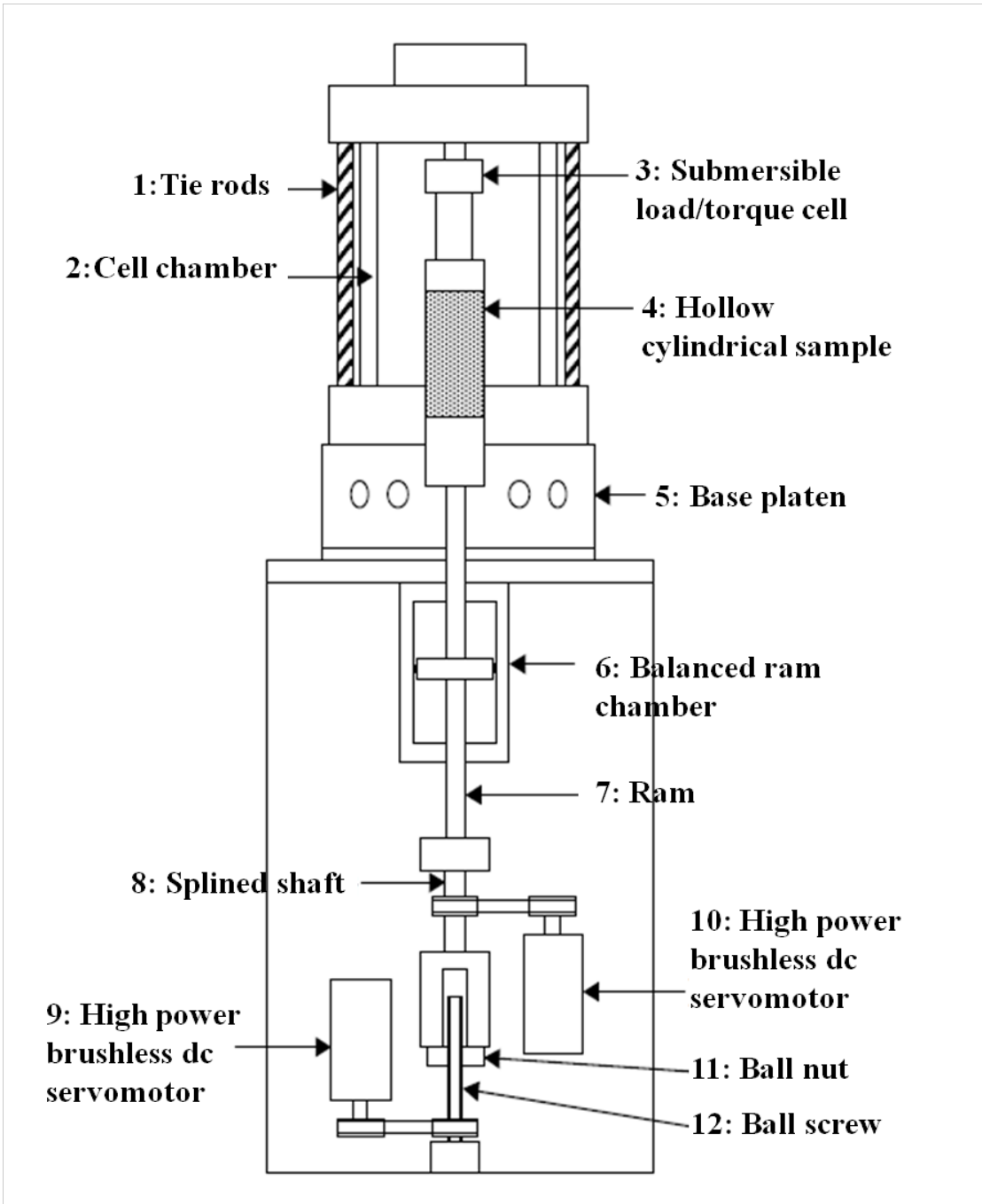

Fig. 1. Schematic cross section of the GDS Hollow Cylinder Apparatus.

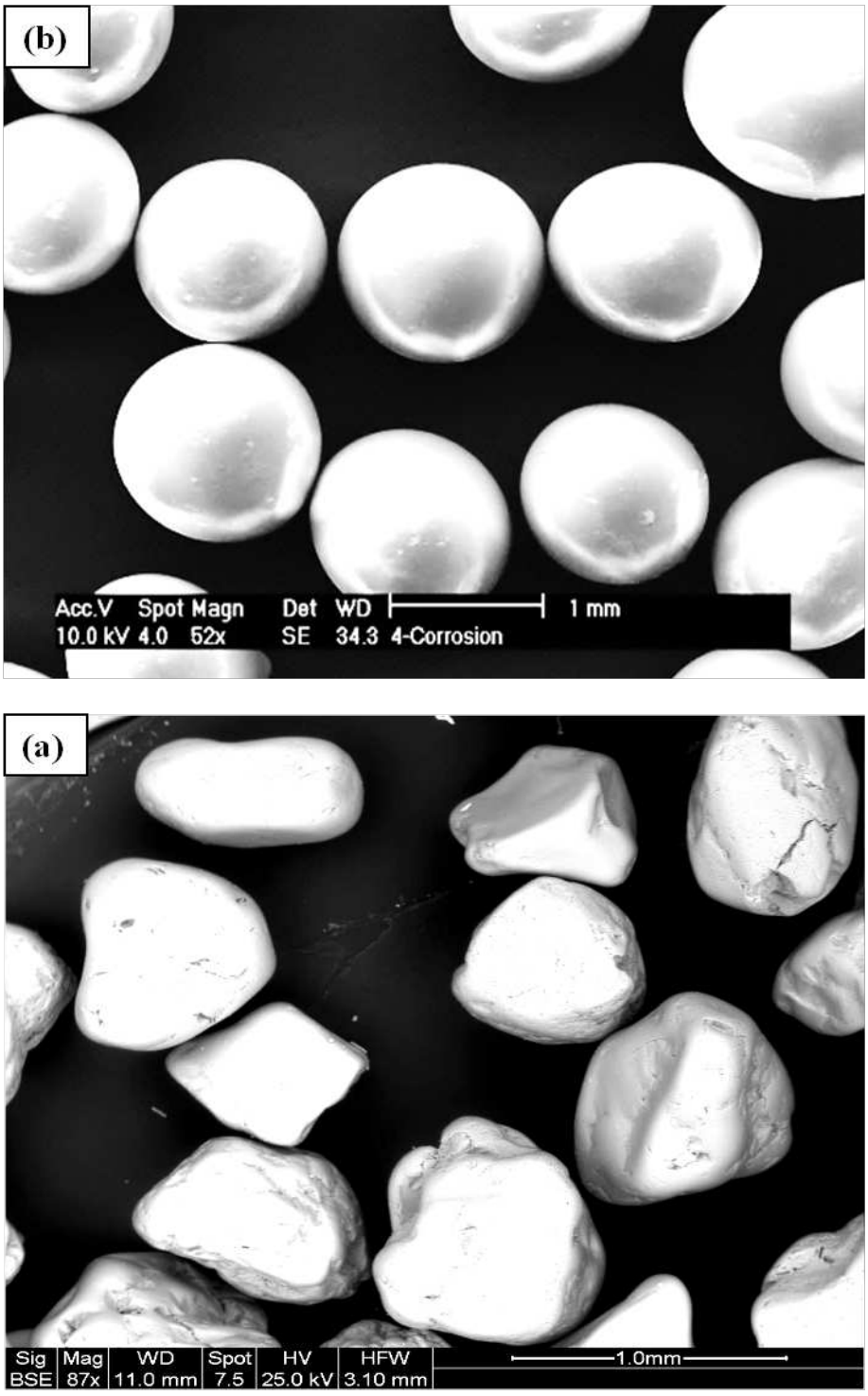

Fig. 2. Scanning electron micrograph of (a) Leighton Buzzard B sand and (b) Ballotini glass beads.

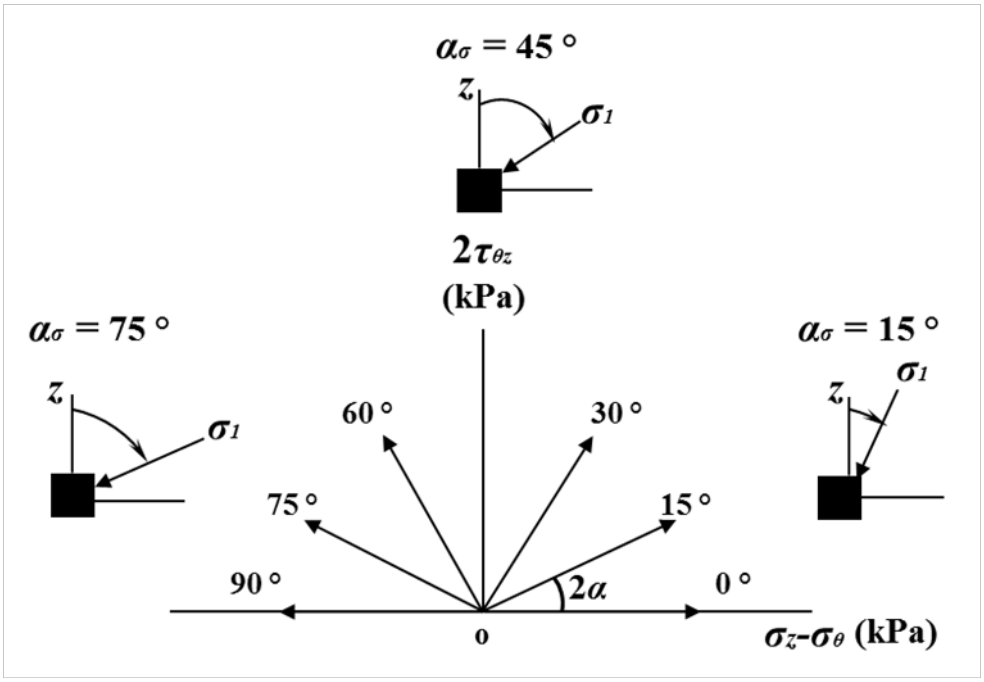

Fig. 3. Stress paths in the X-Y stress space for monotonic loading tests.

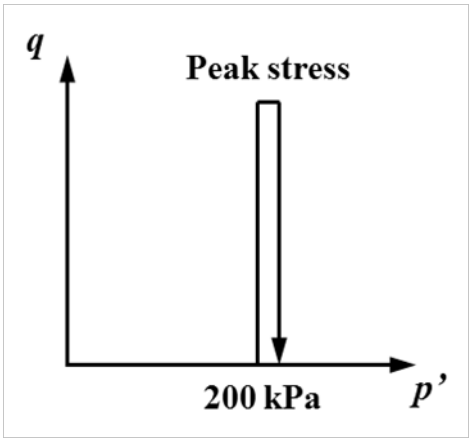

Fig. 4. Designed stress paths in *q-p'* stress space for pre-loading tests.

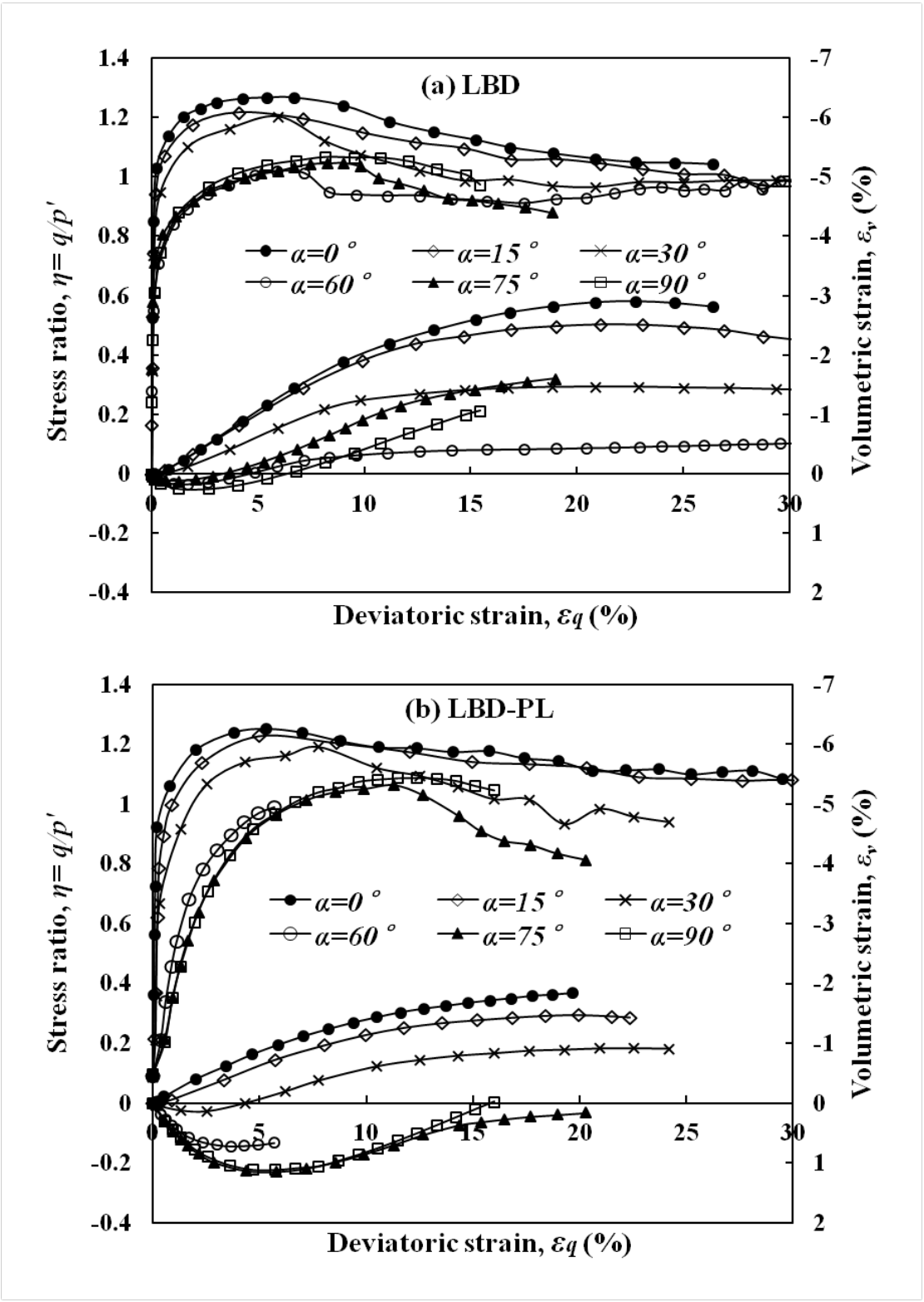

Fig. 5. Stress-strain behaviour at different loading directions for: (a) dense sand; (b) presheared sand.

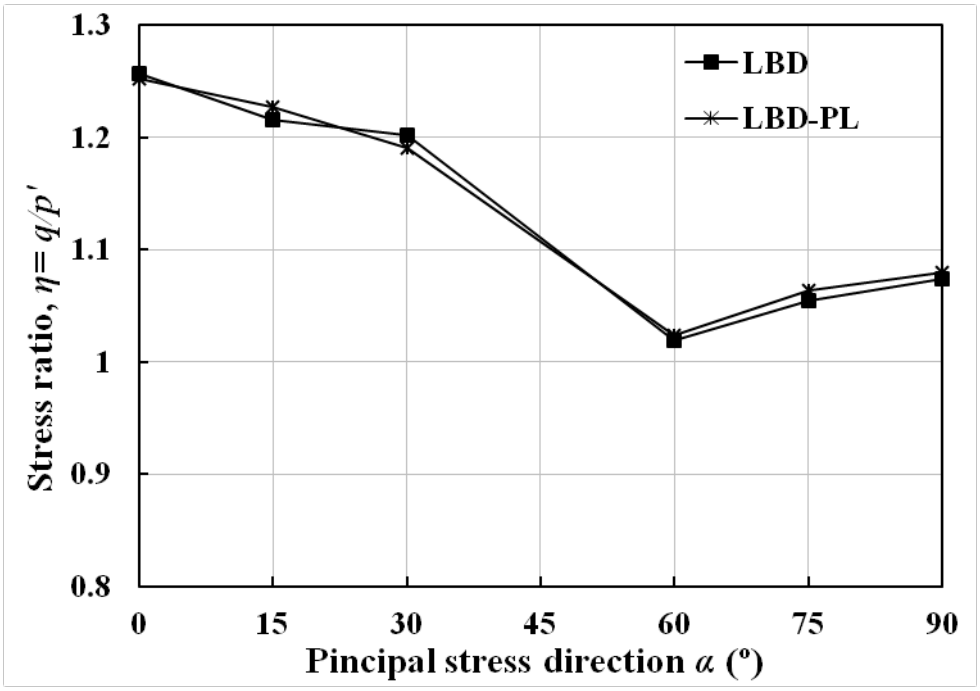

Fig. 6. Comparison of the peak stress ratio obtained at different loading directions between dense sand and presheared sand.

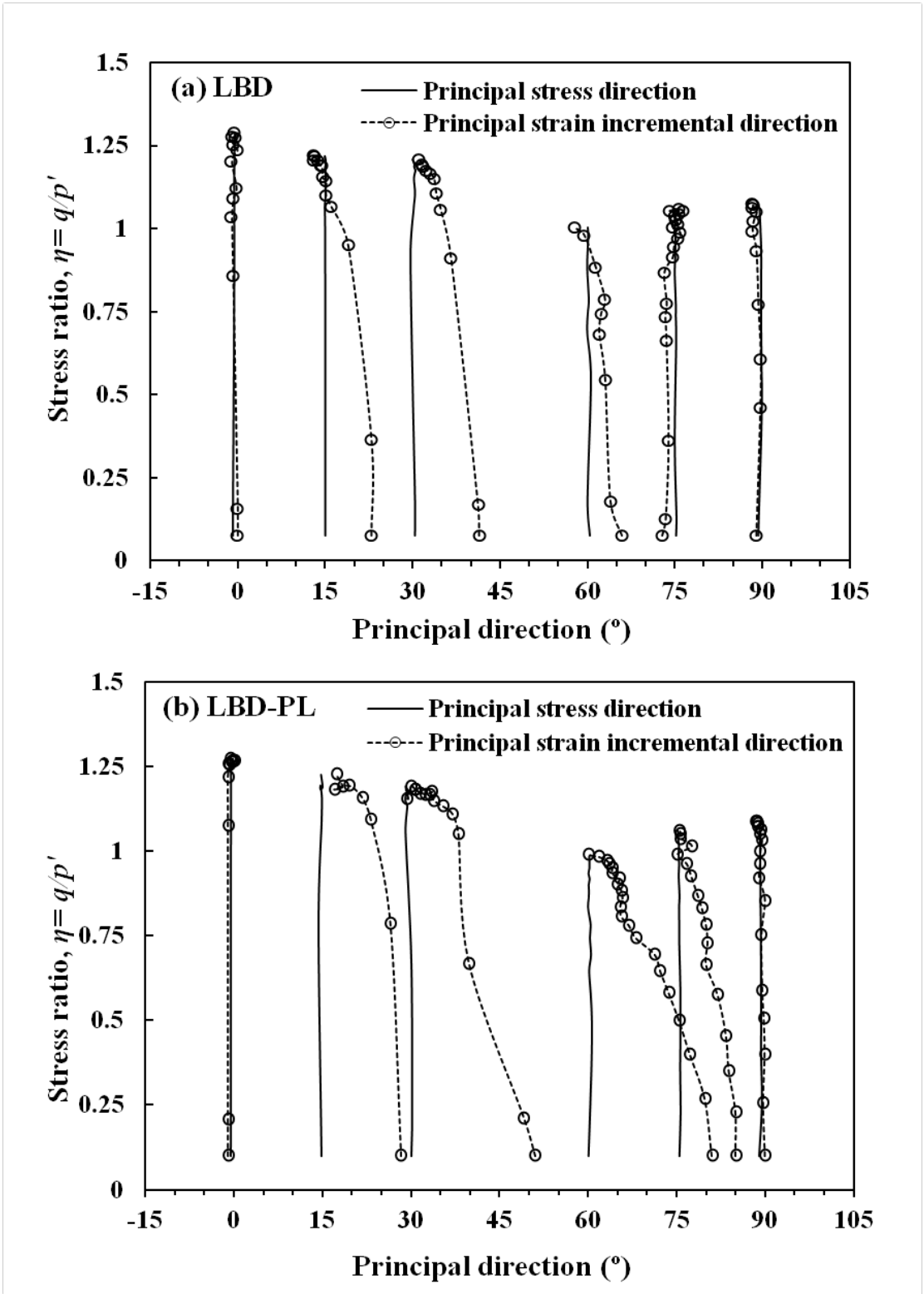

Fig. 7. Stress and strain increment directions at different loading directions for: (a) dense sand; (b) presheared sand.

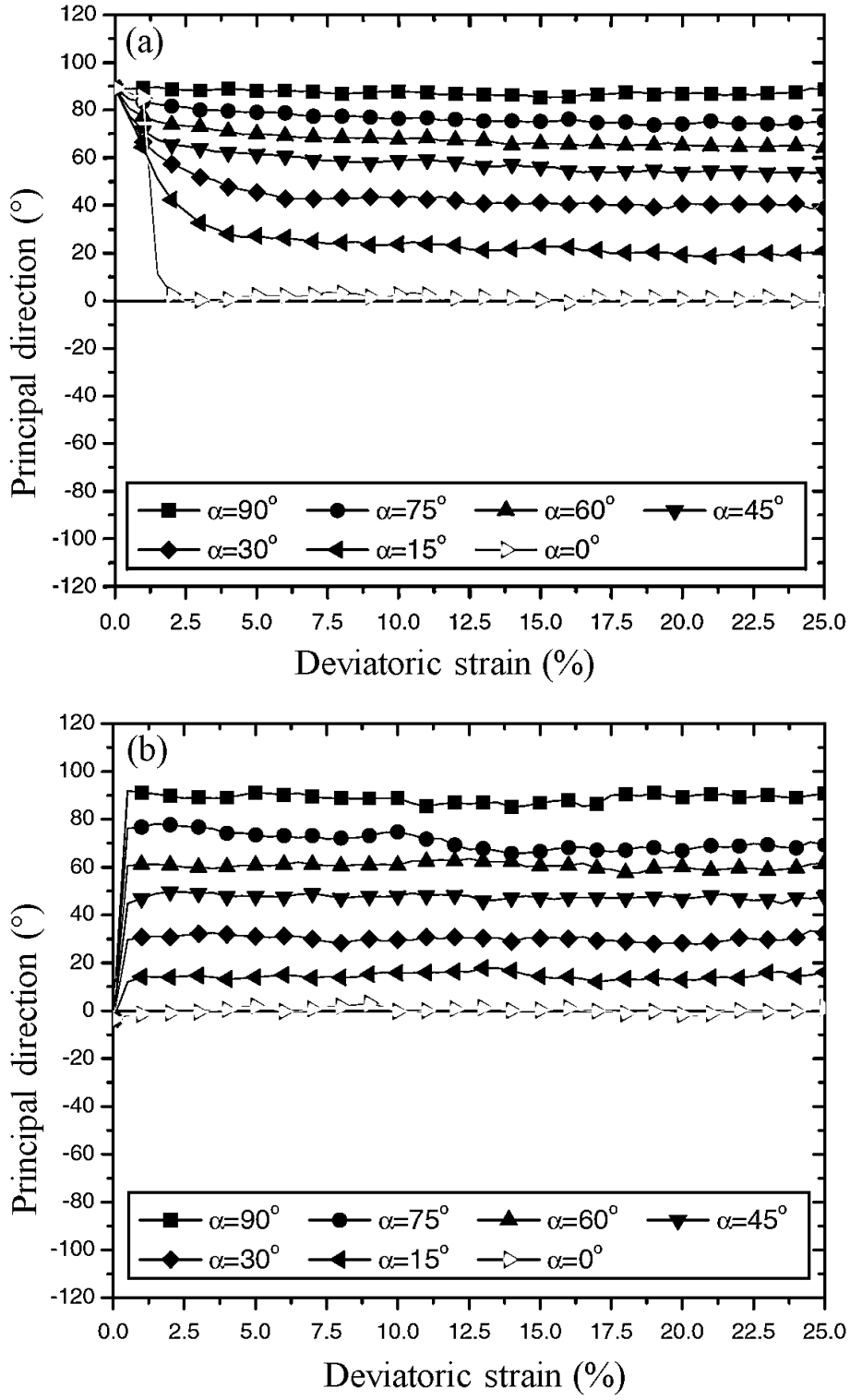

Fig. 8. Principal directions of: (a) fabric anisotropy and (b) contact force anisotropy during monotonic shear in the initially anisotropic sample (after Li and Yu 2009).

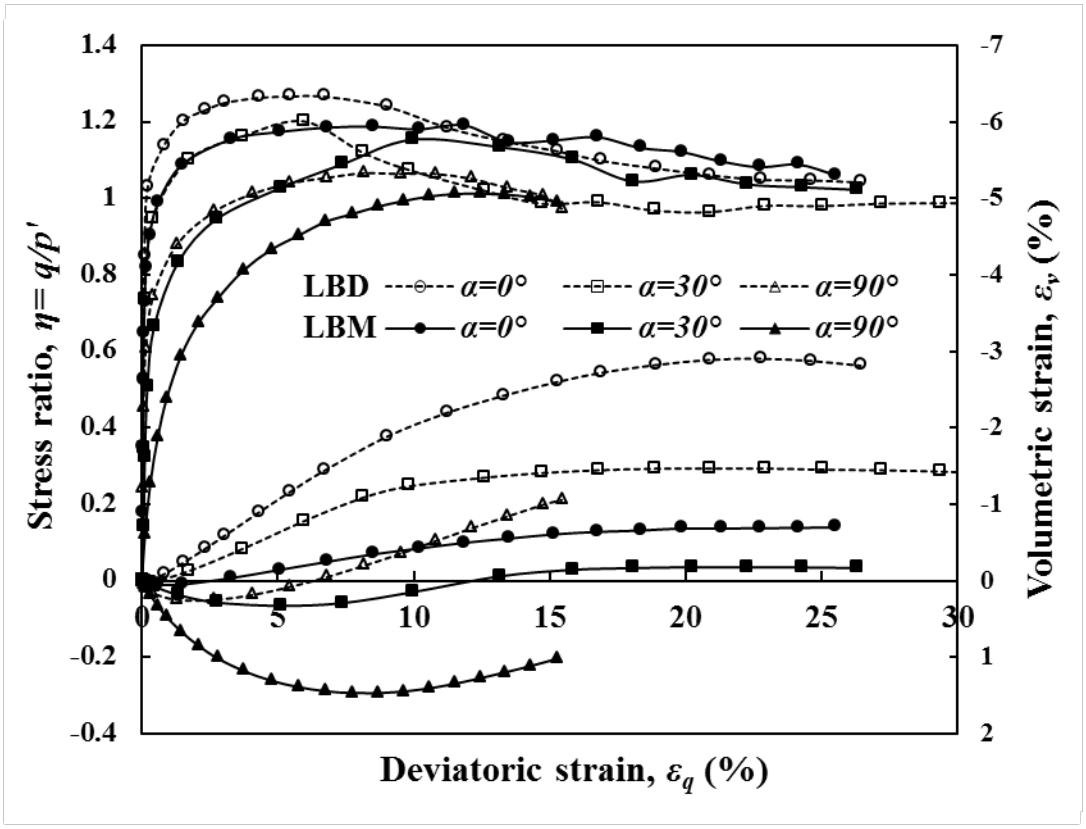

Fig. 9. Comparison of the stress-strain curves obtained at different loading directions between dense sand and medium dense sand.

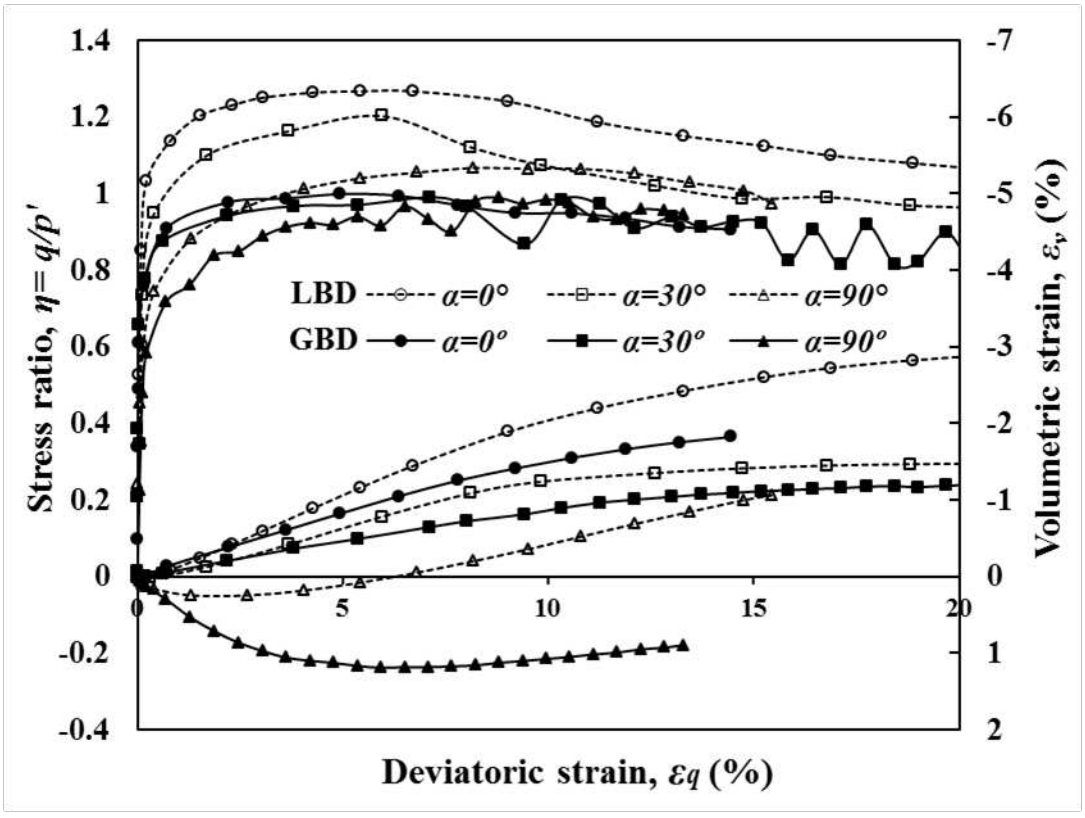

Fig. 10. Comparison of the stress-strain curves obtained at different loading directions between dense sand and glass beads.

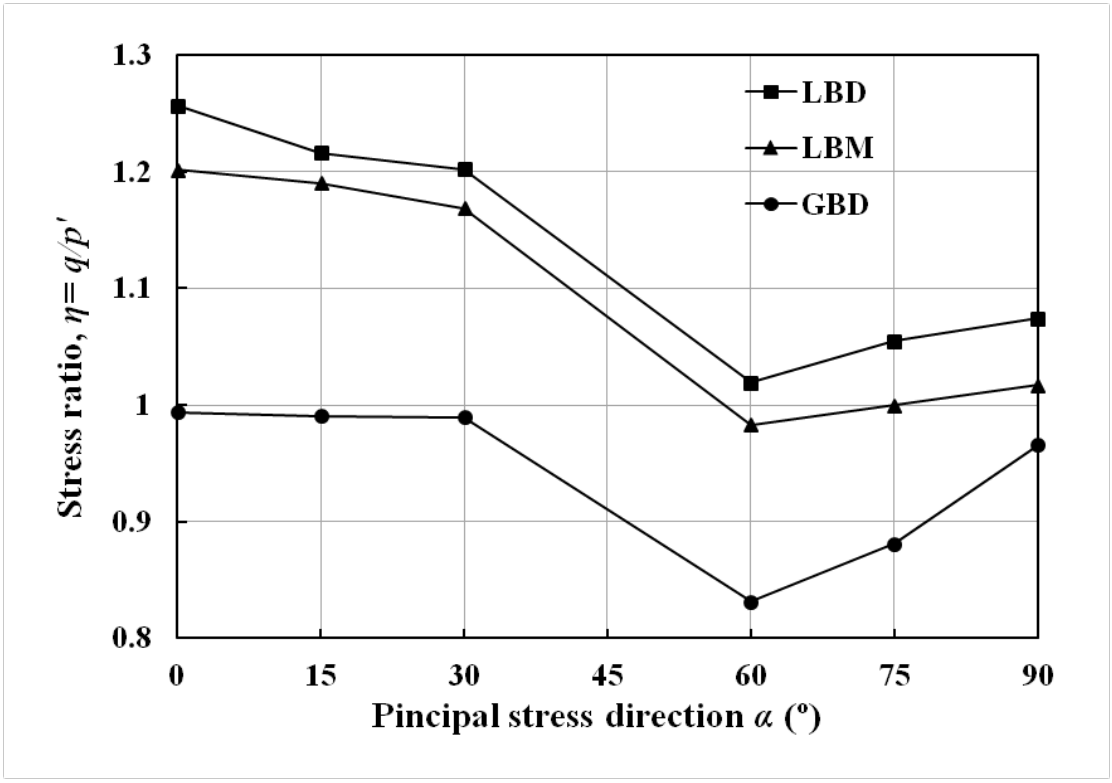

Fig. 11. Comparison of the peak stress ratio obtained at different loading directions between dense sand, medium dense sand and glass beads.

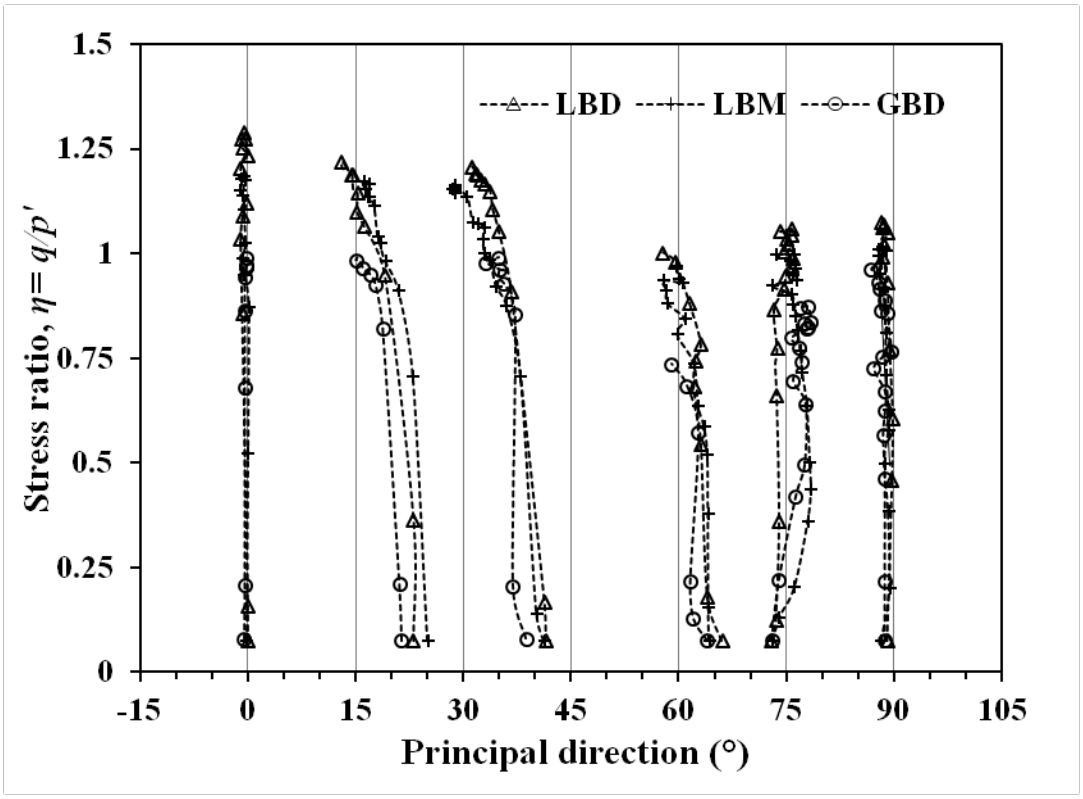

Fig. 12. Comparison of the strain increment directions obtained at different loading directions between dense sand, medium dense sand and glass beads.

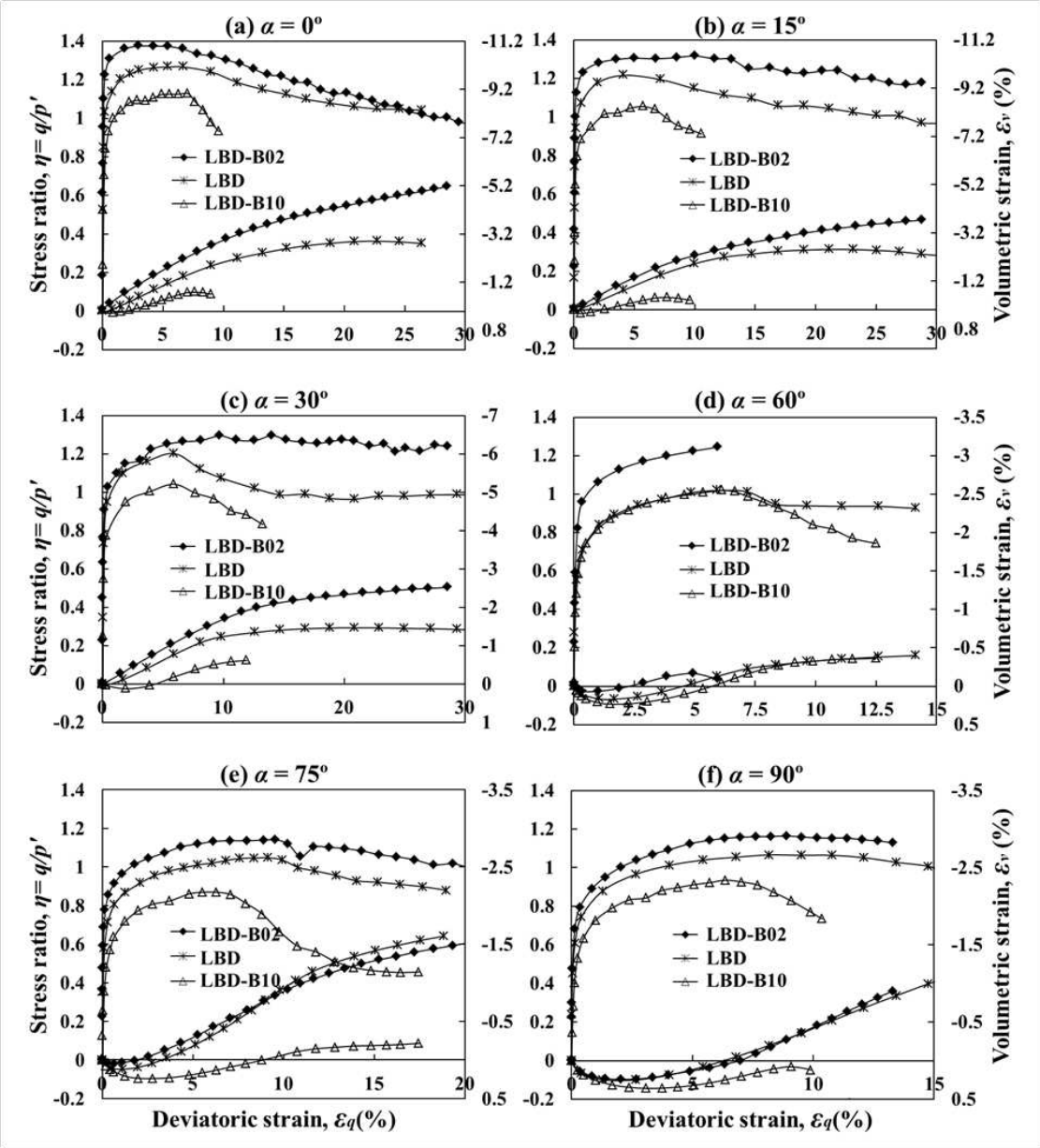

Fig. 13. Stress-strain behaviour at: (a) α = 0º; (b) α = 15º; (c) α =30º; (d) α = 60º; (e) α = 75º; (f) α = 90º for tests with b = 0.2, b = 0.5 and b = 1.0.

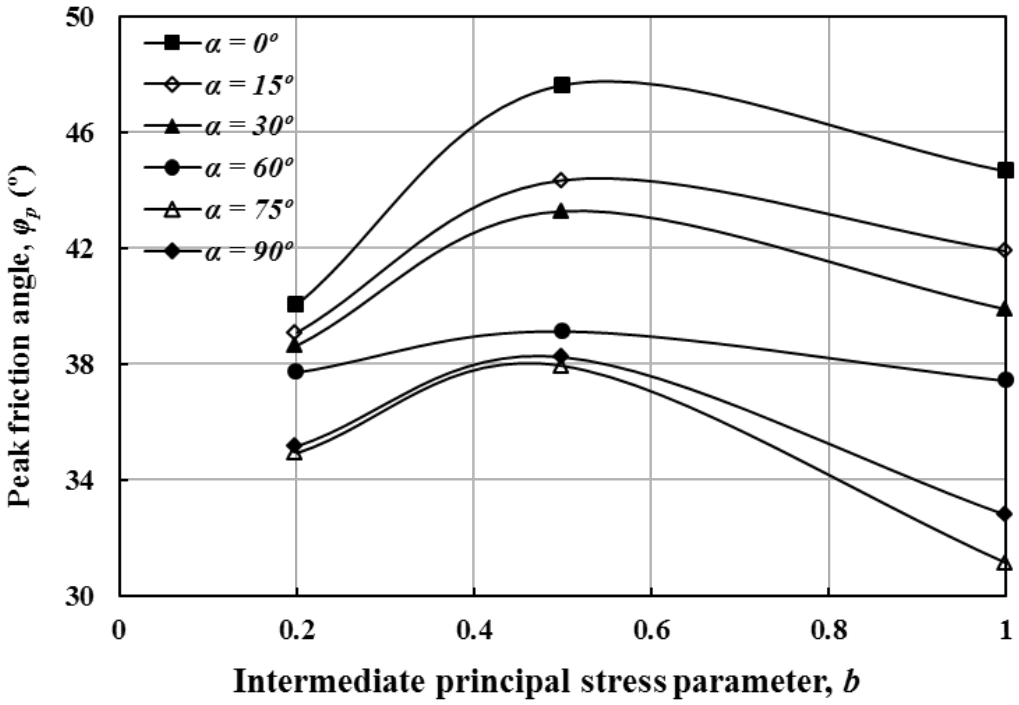

Fig. 14. Peak stress ratio at different major principal stress directions for tests with b = 0.2, b = 0.5 and b = 1.0.

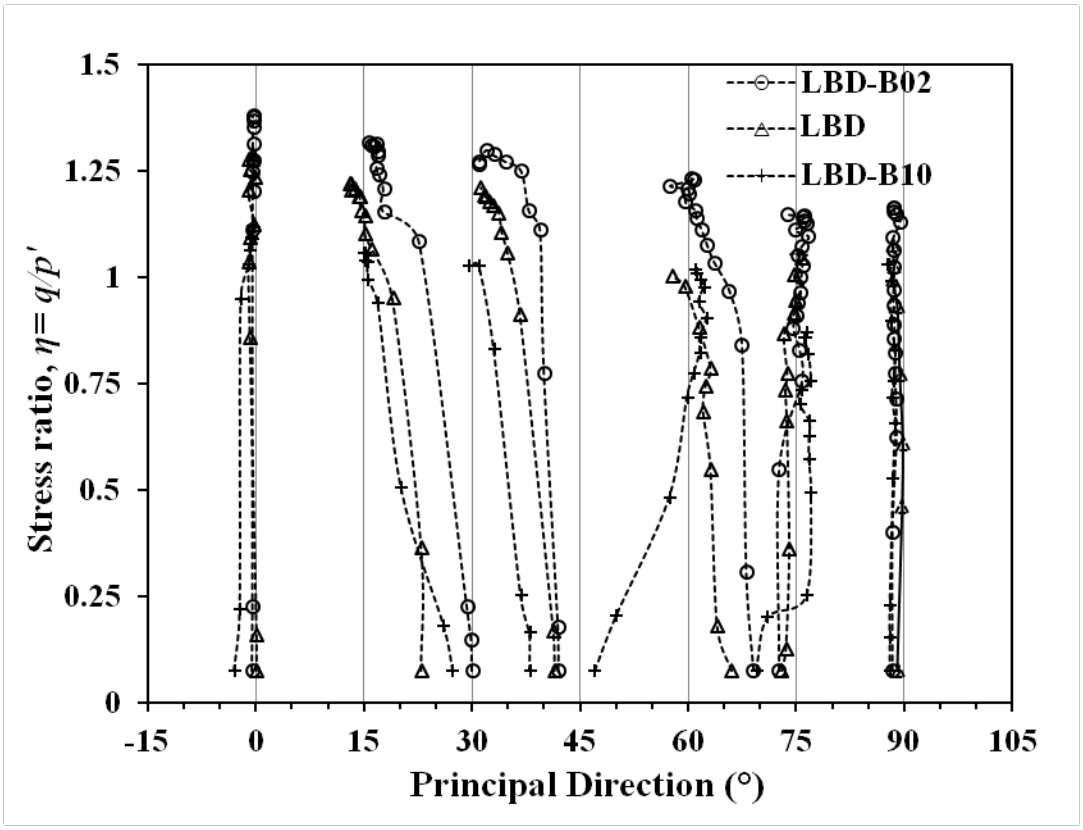

Fig. 15. Comparison of strain increment directions for tests with b = 0.2, b = 0.5 and b =1.0 at: α = 15º, 30º, 60º and 75º.

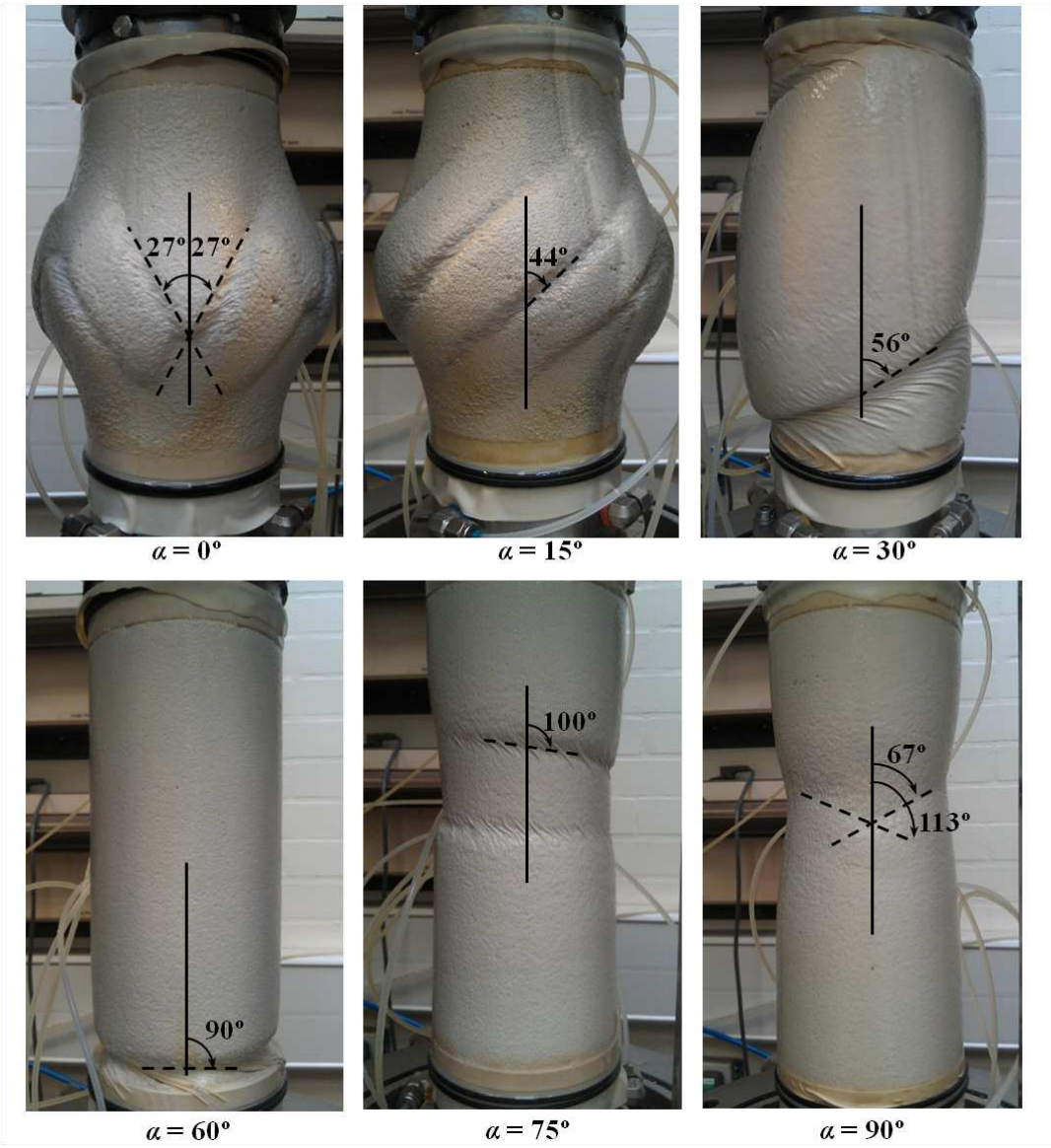

Fig. 16. Shear bands developed in dense sand specimens at different loading directions.

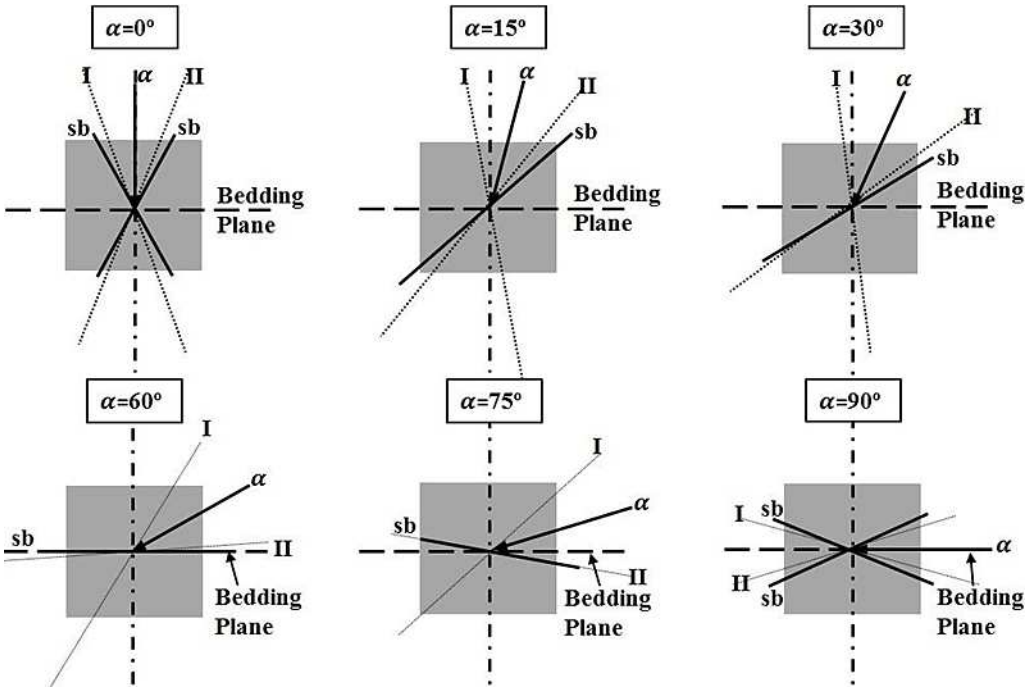

Fig. 17. Comparison of experimental shear band inclinations with theoretical predictions.

Table 1. Physical properties of Leighton Buzzard sand and Ballotini glass beads

Property	Leighton Buzzard Sand	Ballotini glass beads
Mean grain size D_{50}: mm	0.62	1.35
Effective grain size D_{10}: mm	0.45	1.15
Uniformity coefficient Cu: D_{60}/ D_{10}	1.56	1.18
Specific gravity Gs	2.65	2.50
Minimum void ratio e_{min}	0.52	0.52
Maximum void ratio e_{max}	0.79	0.68

Table 2. Initial conditions for monotonic shear tests

Test series	Test No.	D_{rc} (%)	e_c	α (°)	b
Series 1 Dense sand	LBD	76	0.58	0, 15, 30, 60, 75, 90	0.5
Series 2 Medium sand	LBM	43	0.67		0.5
Series 3 Presheared sand	LBD-PL	76	0.58		0.5
		after preshearing			
		73			
Series 4 Different b values	LBD-B02	76	0.58		0.2
	LBD-B10	76	0.58		1.0
Series 5 Ballotini glass beads	GBD	90	0.54		0.5

D_{rc}: relative density after consolidation, e_c: void ratio after consolidation, α: principal stress direction, b: intermediate principal stress parameter.

Table 3. Comparison of experimental shear band inclinations with theoretical predictions

α (°)	0	15	30	60	75	90
α_{sb} (°)	-27, 27 crossed	44 parallel	56 single	90 single	100 single	67,113 crossed
θ_v (°)	-21 (I) 21 (II)	-8 (I) 38 (II)	-7 (I) 53 (II)	33 (I) 87 (II)	49 (I) 101 (II)	64 (I) 116 (II)